
**МИНЕРАЛЫ
И ПАРАГЕНЕЗИСЫ МИНЕРАЛОВ**

**HYDROUS FERRIC SULFATE $\text{Fe}(\text{SO}_4)(\text{OH}) \cdot 2\text{H}_2\text{O}$ FROM THE SUPERGENE ZONE
OF THE KHANGALAS GOLD DEPOSIT, EASTERN YAKUTIA, RUSSIA**

© 2020 г. М. V. Kudrin¹, *, N. V. Zayakina¹, V. Yu. Fridovsky¹, and L. T. Galenchikova¹

¹*Diamond and Precious Metal Geology Institute SB RAS, Lenin st., 39, Yakutsk, 677000 Russia*

**e-mail: kudrinmv@mail.ru*

Received April 12, 2020; Revised April 12, 2020; Accepted May 18, 2020

A hydrous ferric sulfate with a formula $\text{Fe}(\text{SO}_4)(\text{OH}) \cdot 2\text{H}_2\text{O}$ was discovered in the supergene zone of the Khangalas gold ore deposit, Yakutia, Russia. Studies of the mineral showed that it has no analogues among natural and synthetic compounds. The mineral is beige-yellow in color, very soft, with a fibrous texture and a finely crystalline structure. It occurs as veinlets and nest-like aggregates (up to 5–6 cm in size) of thin, elongate, acicular crystals $\leq 1 \mu\text{m}$ across and $\leq 20 \mu\text{m}$ in length. Associated minerals are quartz, jarosite, muscovite, and anorthite. The chemical composition (wet-chemical analysis in wt %) is as follows: Fe_2O_3 37.82, SO_3 37.84, H_2O 22.70, SiO_2 0.26, Al_2O_3 0.38, total 99.00. The empirical formula calculated on the basis of one S atom per formula unit (*apfu*) is $\text{Fe}_{1.002}(\text{SO}_4)(\text{OH}) \cdot (\text{H}_{4.33}\text{O}_{2.18})$. The simplified formula $\text{Fe}(\text{SO}_4)(\text{OH}) \cdot 2\text{H}_2\text{O}$ requires Fe_2O_3 38.96, SO_3 39.07, H_2O 21.97, total 100.00 wt %. The unit-cell parameters were refined by the least squares method for the full X-ray pattern. A triclinic cell with parameters $a = 7.30(1)$, $b = 10.96(2)$, $c = 11.70(2)$ Å, $\alpha = 108(1)^\circ$, $\beta = 102.1(4)^\circ$, $\gamma = 97.0(2)^\circ$, $V = 853(8)$ Å³, $Z = 6$ was chosen from among the various possible variants, space group $P1$, $P\bar{1}$ (?). The strongest X-ray powder diffraction lines [d , Å (I , %) (hkl)] are: 10.72 (100) (001), 10.22 (80) (010), 9.12 (28) (0–11), 5.356 (8) (002), 4.108 (10) (–1–21), 3.758 (9) (1–22), 3.476 (4) (0–32). The mineral is chemically close to polymorphic modifications of the hydrous ferric sulfate $\text{Fe}(\text{SO}_4)(\text{OH}) \cdot 2\text{H}_2\text{O}$: butlerite and parabutlerite, but differs from them in the X-ray powder diffraction pattern and IR and Raman spectra. These facts served as the basis for a detailed study of the mineral. Due to the fine-fibrous texture and poor quality of X-ray diffraction reflections, the crystal structure of the found sulfate has not been resolved. It was the main reason why the mineral was not approved by the Commission on New Minerals and Mineral Names of the International Mineralogical Association (CNMMN, IMA).

Keywords: hydrous ferric sulfate, $\text{Fe}(\text{SO}_4)(\text{OH}) \cdot 2\text{H}_2\text{O}$, butlerite, parabutlerite, X-ray powder diffraction pattern, IR and Raman spectra, supergene zone, permafrost, Khangalas deposit, Yakutia

DOI: 10.31857/S0869605520030120

INTRODUCTION

The territory of Eastern Yakutia within the Verkhoyansk-Kolyma folded system is characterized by a sharply continental, arid climate and the presence of permafrost. These are favourable conditions for preservation of hydrous sulfates of iron, magnesium, aluminium, and zinc, which are often found in deposits in the ores, rocks and their oxidation products. The preservation of such minerals in warm and humid environments could be problematic. Recently, some rare sulfates have been found in the supergene zones of ore deposits in East Yakutia: sanjuanite $\text{Al}_2(\text{PO}_4)(\text{SO}_4)(\text{OH})(\text{H}_2\text{O})_9$ (Lazebnik et al., 1998), arangasite $\text{Al}_2\text{F}(\text{PO}_4)(\text{SO}_4)(\text{H}_2\text{O})_9$ at the Alyaskitovoe deposit, (Gamyarin et al., 2013; Yakubovich et al.,

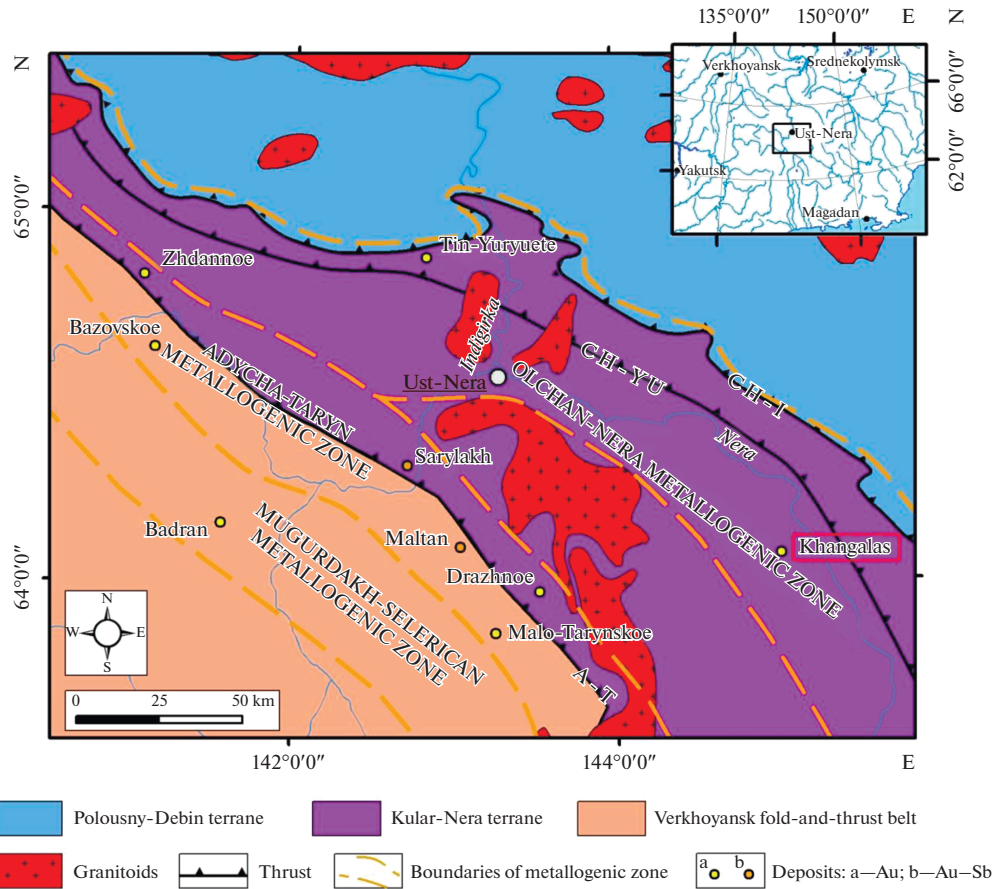


Fig. 1. Regional position of the Khangalass gold deposit (after Fridovsky, 2018 with modifications). Faults: CH-I – Charky–Indigirka, CH – Chay–Yureya, AT – Adycha–Taryn.

Рис. 1. Региональная позиция золоторудного месторождения Хангалас (по: Fridovsky, 2018). Разломы: CH-I – Чаркы-Индибирский, CH – Чай-Юреинский, AT – Адыча-Тарынский.

2014), mangazite $\text{Al}_2(\text{SO}_4)(\text{OH})_4 \cdot 3\text{H}_2\text{O}$ at the Mangazeyskoe deposit (Gamyatin et al., 2007), cranswickite $\text{MgSO}_4 \cdot 4\text{H}_2\text{O}$ at the Malo-Tarynskoe deposit (Zayakina, 2019), halotrichite $\text{Fe}^{2+}\text{Al}_2(\text{SO}_4)_4 \cdot 22\text{H}_2\text{O}$, slavikite $(\text{H}_3\text{O})_3\text{Mg}_6\text{Fe}_{15}^{+3}(\text{SO}_4)_{21}(\text{OH})_{18} \cdot 98\text{H}_2\text{O}$, as well as zincobotryogen $\text{Fe}^{3+}\text{Zn}(\text{SO}_4)_2(\text{OH}) \cdot 7\text{H}_2\text{O}$ and magnesiocopiapite $\text{MgFe}_4^{3+}(\text{OH})_2(\text{SO}_4)_6 \cdot 20\text{H}_2\text{O}$ at the Endybalskoe deposit (Vasileva, Zayakina, 2019). These supergene sulfates are rarely found as monomineral formations, most often they associate with other sulfates and rock-forming minerals. Our mineral with the composition $\text{Fe}(\text{SO}_4)(\text{OH}) \cdot 2\text{H}_2\text{O}$ is, like most ferric sulfates, a weathering product of Fe-sulfides. Pyrite is abundant in the Khangalass deposit in the ore zones and host rocks. Probably, it is the primary ore mineral of the studied ferric sulfate.

Secondary Fe-containing hydrous sulfates, in which group the discovered mineral falls, occur widely in nature. Under the influence of environmental factors such as temperature, relative humidity, pH of the medium, and fugacity of oxygen and sulfur, processes of hydration

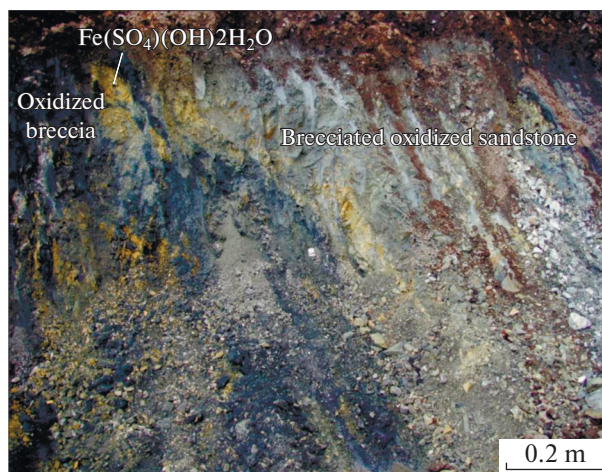


Fig. 2. Location of the find of the mineral $\text{Fe}(\text{SO}_4)(\text{OH}) \cdot 2\text{H}_2\text{O}$ in the trench.

Рис. 2. Расположение находки минерала $\text{Fe}(\text{SO}_4)(\text{OH}) \cdot 2\text{H}_2\text{O}$ в разрезе траншеи.

and dehydration, oxidation and dissolution can readily occur in them. This leads to the formation of other supergene minerals.

In terms of chemical composition ($\text{Fe}_2\text{O}_3 : \text{SO}_3$ ratio close to 1 : 1) the studied mineral belongs to the group of known hydrous ferric sulfates: butlerite, parabutlerite, hohmannite, metahohmannite, amarantite, and fibroferrite. The crystal structures of these sulfates have been solved (Borene, 1970; Fanfani et al., 1971; Scordari, 1978; Scordari, 1981; Scordari et al., 2004; Ventruti et al., 2015; Ventruti et al., 2016a; Ventruti et al., 2016b). All of them are constructed from Fe^{3+} octahedra and SO_4 tetrahedra variously interconnected in chains linked by hydrogen bonds. As noted by Majzlan et al. (2018), two types of crystal structure are realized in this group of sulfates. Amarantite, hohmannite, and metahohmannite have structures with a complex chain, while butlerite, parabutlerite, fibroferrite, and $\text{Fe}(\text{SO}_4)(\text{OH})$ display a simpler chain (Hawthorne et al., 2000) with variations in packing. Thermodynamic characteristics of hydrous ferric sulfates, conditions of their formation, phase stability fields, and a new structural model of amarantite are considered in detail in a paper by Majzlan et al., (2018), wherein a diagram of successive transitions from the most highly hydrated sulfate fibroferrite $\text{Fe}(\text{SO}_4)(\text{OH})(\text{H}_2\text{O})_5$ to butlerite $\text{Fe}(\text{SO}_4)(\text{OH})(\text{H}_2\text{O})_2$ to $\text{Fe}(\text{SO}_4)(\text{OH})$ during dehydration is also given. The process of dehydration passes through a series of phases of unknown nature. Another point of interest is the position of the mineral we found within the group of known hydrous ferric sulfates, and whether it is yet another polymorphic modification of butlerite and parabutlerite.

MATERIALS AND METHODS

The studied hydrous ferric sulfate $\text{Fe}(\text{SO}_4)(\text{OH}) \cdot 2\text{H}_2\text{O}$ was found in 2014 in the supergene zone of the Khangalas gold ore deposit, in the headwaters of the Levyi Khangalas creek, a left-side tributary of the Nera River, Yakutia, North-East Russia (Lat. $64^\circ 05' 58''$ N, Long. $144^\circ 55' 02''$ E) (Fig. 1). The Khangalas deposit is an orogenic type deposit, with a low-sulfide gold-quartz mineralization. The amount of ore minerals does not exceed 1–3%, they are represented mainly by arsenopyrite, pyrite, galena, sphalerite, chalcopyrite, native gold with an average fineness of 820–830‰, and, less often, by antimonite and lead sulfosalts (boulangerite). Quartz is the main vein mineral, with less common carbonates (calcite, siderite)



Fig. 3. Sample of mineral $\text{Fe}(\text{SO}_4)(\text{OH}) \cdot 2\text{H}_2\text{O}$.

Рис. 3. Образец минерала $\text{Fe}(\text{SO}_4)(\text{OH}) \cdot 2\text{H}_2\text{O}$.

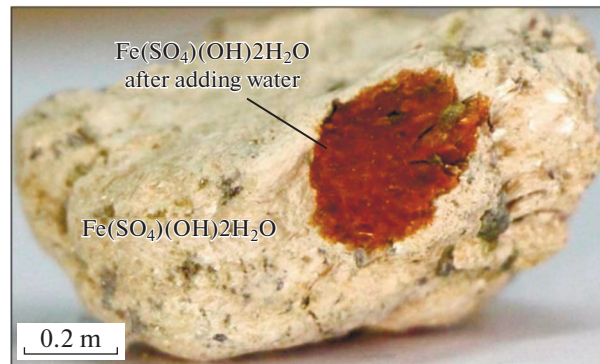


Fig. 4. Appearance of the mineral $\text{Fe}(\text{SO}_4)(\text{OH}) \cdot 2\text{H}_2\text{O}$ after adding water on the surface.

Рис. 4. Облик минерала $\text{Fe}(\text{SO}_4)(\text{OH}) \cdot 2\text{H}_2\text{O}$ после добавления воды на его поверхность.

and chlorite (Fridovsky et al. 2018; Kudrin, 2018). It should be noted that the ore zones and host rocks of the deposit underwent strong exogenous changes, as evidenced by the development of Fe hydroxides, arsenates, and sulfates (Kudrin et al., 2018, 2019).

The mineral $\text{Fe}(\text{SO}_4)(\text{OH}) \cdot 2\text{H}_2\text{O}$ was first found in a freshly dug trench at a depth of 1.5–2 m from the surface in association with quartz, jarosite, muscovite, and anorthite (Fig. 2). It is beige-yellow in color, very soft, with a fibrous texture and a finely crystalline structure. It forms veinlets and nest-like aggregates (up to 5–6 cm in size) of elongate acicular crystals $\leq 1 \mu\text{m}$ across and $\leq 20 \mu\text{m}$ in length (Figs. 3–5). The mineral is prone to hydrolysis, it tends to oxidize in moist conditions to lose its original shape, structure, and color (Fig. 4). The crystals are water soluble, their good state of preservation is due, as in the case of other hydrous sulfates found in Yakutia, to specific climatic conditions. The unpowdered samples remained unchanged in laboratory conditions for 5 years, as evident from X-ray diffraction patterns recorded regularly since 2014. The powdery material gradually changed its colour from brownish to red-brown. Their diffraction lines become diffuse with low intensities.

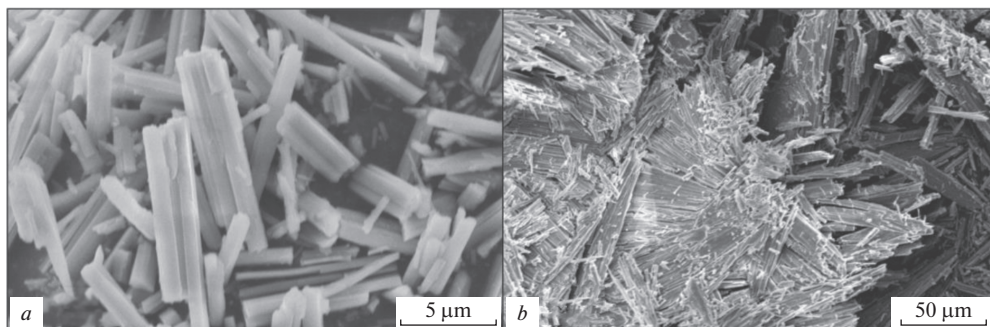


Fig. 5. Parallel (*a*) and sheaf-like (*b*) clusters of fine granular acicular crystals of sulfate $\text{Fe}(\text{SO}_4)(\text{OH}) \cdot 2\text{H}_2\text{O}$. SEM images.

Рис. 5. Параллельные (*a*) и сноповидные (*b*) сростки тонкоигольчатых кристаллов сульфата $\text{Fe}(\text{SO}_4)(\text{OH}) \cdot 2\text{H}_2\text{O}$. Изображения в обратно-отраженных электронах.

The elementary composition and morphology of the crystals were determined using a JEOL JSM-6480LV scanning electron microscope equipped with an Oxford INCA 350 energy-dispersive spectrometer (20 kV, 1 nA, beam diameter 1 μm) (analyst A.V. Popov, DPMGI, Yakutsk). It was found that the mineral samples are easily destructible under the electron microscope rays.

The classical wet chemical method was used to determine the chemical composition of the mineral. Two samples were analysed and the formula was calculated on the basis of averaged analytical data. The water content, determined by the Penfield method, is close to the results of the thermal analysis. Three assays (100 to 170 mg in weight) were taken from each sample and the data obtained were averaged. Sulfur content was determined from two assays (350 to 500 mg) for each sample.

The pXRD analysis of the found sulfate and associated minerals was carried out with a Bruker D2 PHASER diffractometer operated at 30 kV and 10 mA, with CuK_α radiation, in the range (2θ) of 4° – 65° . The PDF-2 database was used. The mineral crystals were handpicked under a binocular microscope and ground in an agate mortar without adding alcohol or water. Five sulfate samples taken at different times were studied. The small size and poor quality of the crystals did not allow obtaining suitable experimental material for determining the crystal structure. Even the use of synchrotron radiation (Yu Sheng, Argonne National Laboratory, USA) was ineffective. An attempt to solve the crystal structure from the powder data at the X-Ray Diffraction Centre of Saint Petersburg State University, Russia, was unsuccessful either. We were able to obtain an X-ray oscillation pattern for a crystal intergrowth in the RKOP camera, CuK_α radiation. The use of electron microscopy to determine crystallographic parameters is very problematic, since the studied sulfate is a highly hydrated compound and easily loses water with the destruction of the crystal structure.

The IR spectrum of the sulfate was recorded with an IR Fourier Protégé 40 spectrometer using a standard pelletization technique (analyst I.N. Zueva). The thermograms of the mineral were obtained using a NETZSCH STA 449 C Jupiter thermal analyzer; weight of samples from 9.59 to 12.95 mg, heating rate $10^\circ/\text{min}$, Ar atmosphere (analyst N.N. Emelyanova). Six samples were tested.

The Raman spectrum of the sulfate was obtained with the use of the INTEGRA SPEKTR measuring system, analyst V.I. Popov, Ammosov North-Eastern Federal University. Operating conditions: $100\times$ objective with numerical aperture $\text{NA} = 0.7$, low-noise CCD camera

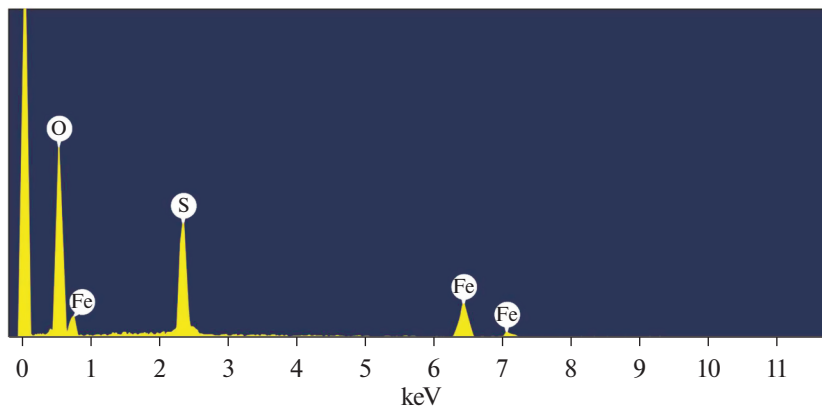


Fig. 6. EDS spectrum of the mineral $\text{Fe}(\text{SO}_4)(\text{OH}) \cdot 2\text{H}_2\text{O}$.

Рис. 6. EDS спектр минерала $\text{Fe}(\text{SO}_4)(\text{OH}) \cdot 2\text{H}_2\text{O}$.

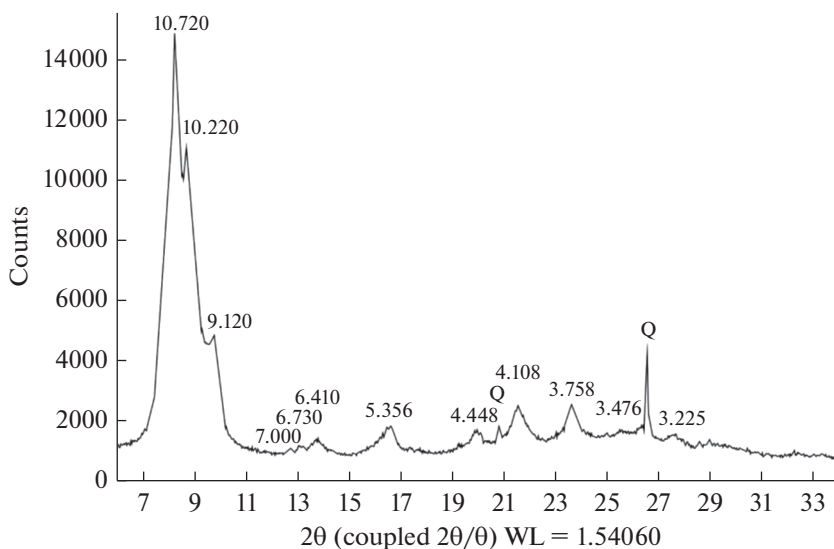


Fig. 7. Fragment of the X-ray powder pattern for $\text{Fe}(\text{SO}_4)(\text{OH}) \cdot 2\text{H}_2\text{O}$. Q – quartz.

Рис. 7. Фрагмент рентгенограммы $\text{Fe}(\text{SO}_4)(\text{OH}) \cdot 2\text{H}_2\text{O}$. Q – кварц.

with cooling down to -70°C , signal acquisition time at each point 50 s, laser excitation wavelength 532 nm, beam diameter $<1 \mu\text{m}$, power 3.5 mW.

RESULTS

The EDS qualitative analysis made with the use of a JEOL JSM-6480 LV scanning electron microscope showed no elements to be present other than Fe, S, and O (Fig. 6). Chemical data for the studied sulfate are given in Table 1. The empirical formula (based on one S *apfu*) is

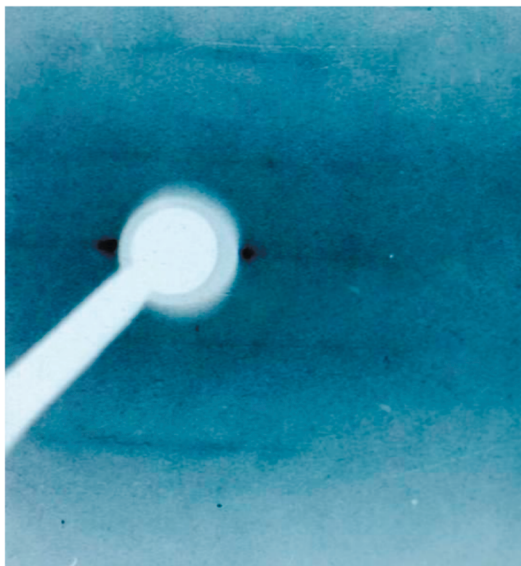


Fig. 8. X-ray oscillation pattern for intergrowth crystals of $\text{Fe}(\text{SO}_4)(\text{OH}) \cdot 2\text{H}_2\text{O}$.

Рис. 8. Рентгенограмма качания для сростков кристаллов $\text{Fe}(\text{SO}_4)(\text{OH}) \cdot 2\text{H}_2\text{O}$.

$\text{Fe}_{1.002}(\text{SO}_4)(\text{OH}) \cdot (\text{H}_{4.33}\text{O}_{2.18})$. The simplified formula is $\text{Fe}(\text{SO}_4)(\text{OH}) \cdot 2\text{H}_2\text{O}$, which requires (wt %): Fe_2O_3 38.96, SO_3 39.07, H_2O 21.97, total 100.00.

All obtained diffraction patterns of the mineral are close to each other and display broad lines. An example of a typical diffractogram is shown in Fig. 7. Figure 8 shows the X-ray oscillation pattern for intergrowth crystals of $\text{Fe}(\text{SO}_4)(\text{OH}) \cdot 2\text{H}_2\text{O}$ from which the unit-cell parameter on elongation of the crystal was estimated. It is equal to or multiple of 7.5 \AA . The averaged X-ray powder diffraction data are listed in Table 2. The calculated values of interplanar distances (d) only closest to the experimental ones are given. The unit-cell parameters were refined using the least squares method over the entire diffractogram. Programs IND and PARAM PDWin of NPP Burevestnik were used to determine the parameters. A triclinic cell with parameters $a = 7.30(1) \text{ \AA}$, $b = 10.96(2) \text{ \AA}$, $c = 11.70(2) \text{ \AA}$, $\alpha = 108(1)^\circ$, $\beta = 102.1(4)^\circ$, $\gamma = 97.0(2)^\circ$, $V = 853(8) \text{ \AA}^3$, $Z = 6$ was chosen from among the various possible variants. When choosing a unit cell, it was taken into account that one parameter is close to the data obtained

Table 1. Chemical composition (wt %) of the mineral $\text{Fe}(\text{SO}_4)(\text{OH}) \cdot 2\text{H}_2\text{O}$
Таблица 1. Химический состав (мас. %) минерала $\text{Fe}(\text{SO}_4)(\text{OH}) \cdot 2\text{H}_2\text{O}$

Constituent	Mean content	Range
Fe_2O_3	37.82	37.71–37.93
SO_3	37.84	37.64–38.04
H_2O	22.70	22.49–22.91
SiO_2	0.26	0.11–0.41
Al_2O_3	0.38	0.24–0.52
Total	99.0	98.19–99.81

Table 2. X-ray powder diffraction data for the mineral $\text{Fe}(\text{SO}_4)(\text{OH}) \cdot 2\text{H}_2\text{O}$
Таблица 2. Данные порошковой рентгенографии для минерала $\text{Fe}(\text{SO}_4)(\text{OH}) \cdot 2\text{H}_2\text{O}$

<i>I</i>	$d_{\text{meas}}, \text{Å}$	$d_{\text{calc}}, \text{Å}$	<i>hkl</i>
100	10.72	10.74	001
80	10.22	10.22	010
28	9.12	9.14	0–11
1	7.00	6.99	100
3	6.73	6.72	–101
3	6.410	6.402	1–10
8	5.356	5.369	002
2	4.599	4.588	1–20
3	4.448	4.445	1–21
10	4.108	4.111	–1–21
9	3.758	3.752	1–22
4	3.476	3.466	0–32
3	3.384	3.397	1–31
3	3.225	3.220	2–11
1	3.117	3.121	210
2	3.067	3.065	–1–31
2	3.030	3.031	1–23
1	2.759	2.761	–104
1	2.653	2.651	–123
2	2.143	2.143	1–52

from the X-ray oscillation pattern for intergrowth crystals. In addition, a good agreement is obtained between the calculated and measured mineral density.

The IR spectrum of the studied sulfate is shown in Fig. 9, *a*. Only the butlerite spectrum is given for comparison (Fig. 9, *b*), since the IR spectra of butlerite and parabutlerite are similar (Cejka et al., 2011). Peaks at 3386, 1622, 1198, 1155, 1086, 1062, 1016, 826, 675, 584, 516, and 419 cm^{-1} are recorded. By analogy with the IR spectra for butlerite and parabutlerite, the broad asymmetric peak at 3386 cm^{-1} can be related to vibrations of H_2O molecules and OH-groups, the 1622 cm^{-1} peak is due to vibration of H_2O molecules, other peaks may correspond to vibrations in the tetrahedral anionic complexes $(\text{SO}_4)^{2-}$.

A typical thermogram is shown in Fig. 10. It should be noted that the thermogram obtained by us differs from those given for butlerite and parabutlerite, perhaps due to the different conditions for obtaining thermograms (Césborn, 1964). Endothermic effects are distinct on the TGA-DTA curves at 119, 255, 694 °C, and an exothermic effect is recorded at 553 °C. A very slight endothermic effect is registered at 344 °C. Analysis of the thermograms showed changes in the weight-loss from 1.5 to 3 wt % at different peaks and a temperature shift up to 10 °C for all peaks except the small peak at 344 °C falling into the interval from 324 to 345 °C.

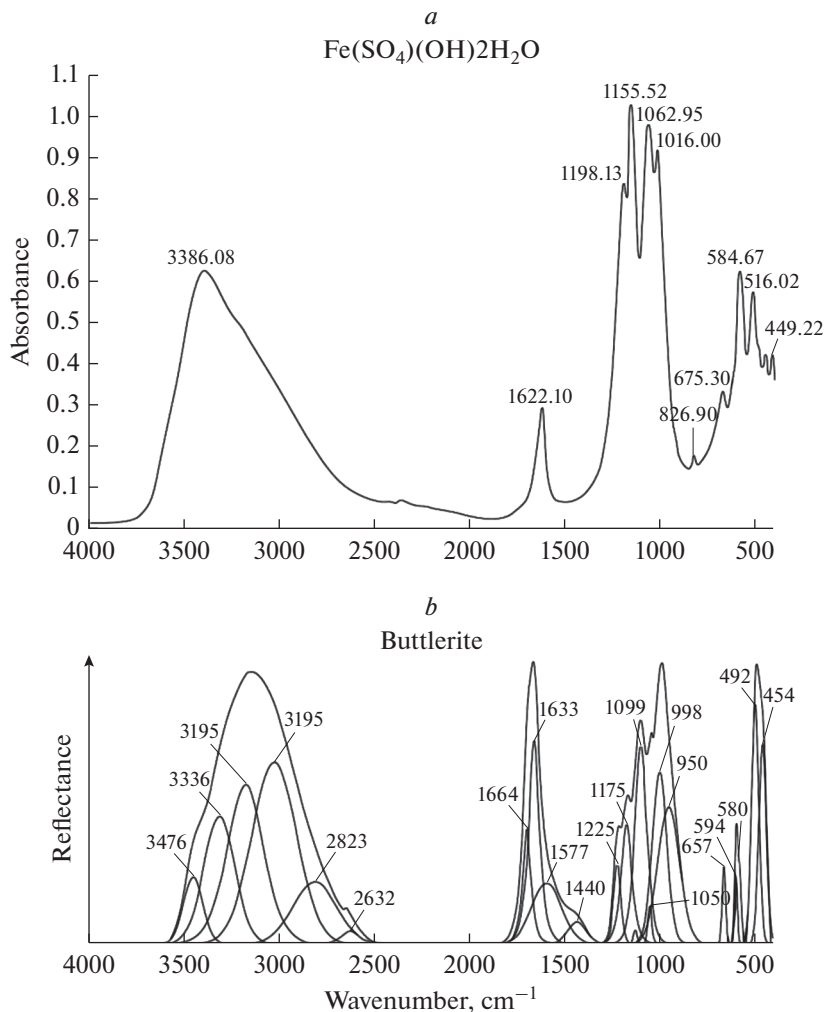


Fig. 9. IR spectra of the mineral (SO₄)(OH) · 2H₂O (*a*) and butlerite (*b*) (Cejka et al., 2011).

Рис. 9. ИК-спектры минерала Fe(SO₄)(OH) · 2H₂O (*a*) и бутлерита (*b*) (Cejka et al., 2011).

The total weight-loss, when heating up to 1000 °C, is 61.58%. On heating from 100 to 450 °C, the weight-loss interpreted as resulting from the loss of water and hydroxyl group of 23.36%, which is close to the amount of water determined by chemical analysis. The exothermic peak at 553 °C relates to the formation of the anhydrous sulfates Fe₂(SO₄)₃ and Fe₁₂S₁₁O₅₁, which have similar X-ray powder patterns. The endothermic peak at 700 °C corresponds to the decomposition of the sulfate and the formation of hematite, which is also confirmed by the X-ray powder patterns.

For comparison with butlerite and parabutlerite, we performed Raman spectroscopy of the discussed ferric sulfate, which revealed its individuality (Fig. 11).

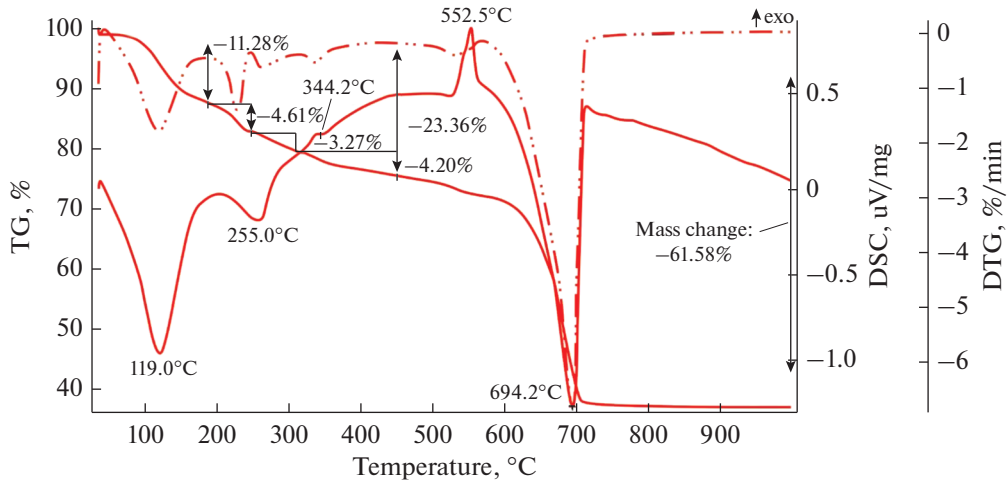


Fig. 10. Thermogram of $\text{Fe}(\text{SO}_4)(\text{OH}) \cdot 2\text{H}_2\text{O}$.

Рис. 10. Термограмма $\text{Fe}(\text{SO}_4)(\text{OH}) \cdot 2\text{H}_2\text{O}$.

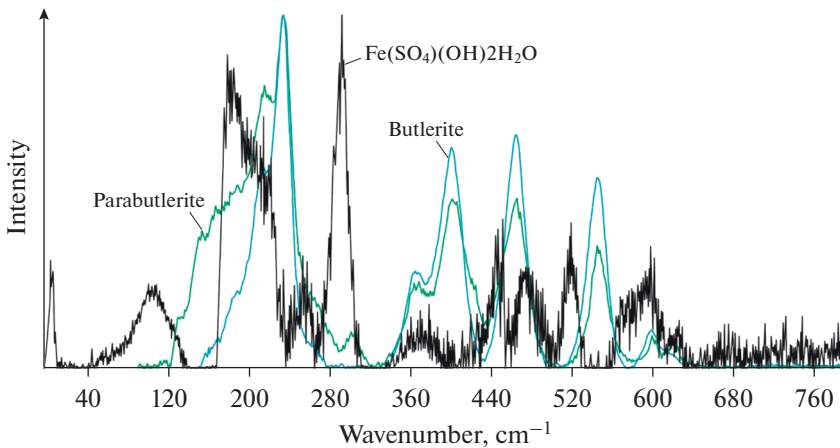


Fig. 11. Raman spectra of the mineral $\text{Fe}(\text{SO}_4)(\text{OH}) \cdot 2\text{H}_2\text{O}$, butlerite (<http://ruff.info>) and parabutlerite (<http://ruff.info>).

Рис. 11. Рамановский спектр минерала $\text{Fe}(\text{SO}_4)(\text{OH}) \cdot 2\text{H}_2\text{O}$, бутлерита (<http://ruff.info>) и парабутлерита (<http://ruff.info>).

DISCUSSION

The paper gives a full description of the secondary hydrous ferric sulfate $\text{Fe}(\text{SO}_4)(\text{OH}) \cdot 2\text{H}_2\text{O}$ which is chemically similar to butlerite and parabutlerite. However, it differs from these polymorphs in its physical characteristics and the X-ray powder patterns. It also has no analogues either among synthetic compounds or minerals with a Fe : S ratio of 1 : 1 (Table 3). A compositionally similar ferric sulfate dihydrate was obtained by Ventruti et al. (2016a) while studying

Table 3. Comparative data for the mineral $\text{Fe}(\text{SO}_4)(\text{OH}) \cdot 2\text{H}_2\text{O}$, butlerite, parabutlerite, hohmannite, metabohmannite, and amaranthite


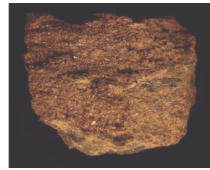
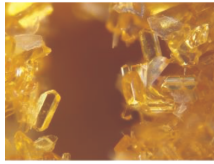
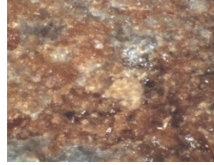

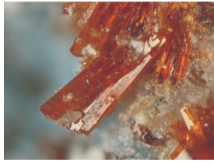
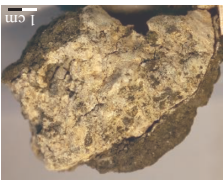
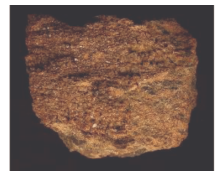
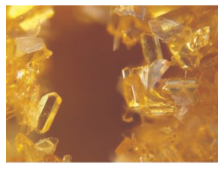
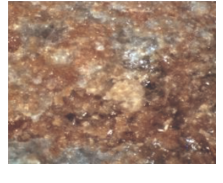


	$\text{Fe}(\text{SO}_4)(\text{OH}) \cdot 2\text{H}_2\text{O}$ This study	Butlerite (Anthony et al., 2003)	Parabutlerite (Anthony et al., 2003)	Hohmannite (Scordari, 1978)	Metabohmannite (Scordari et al., 2004)	Amaranthite (Anthony et al., 2003)
Photo						
Simplified formula	$\text{Fe}(\text{SO}_4)(\text{OH}) \cdot 2\text{H}_2\text{O}$	$\text{Fe}(\text{SO}_4)(\text{OH}) \cdot 2\text{H}_2\text{O}$	$\text{Fe}(\text{SO}_4)(\text{OH}) \cdot 2\text{H}_2\text{O}$	$\text{Fe}_2(\text{O}(\text{SO}_4)_2) \cdot 8\text{H}_2\text{O}$	$\text{Fe}_2(\text{O}(\text{SO}_4)_2) \cdot 4\text{H}_2\text{O}$	$\text{Fe}_2(\text{O}(\text{SO}_4)_2) \cdot 7\text{H}_2\text{O}$
Crystal system	Triclinic	Monoclinic	Orthorhombic	Triclinic	Triclinic	Triclinic
Space group	$P 1, P \bar{1} (?)$	$P21/m(11)$	$Pmnb(62)$	$P \bar{1}$	$P \bar{1}$	$P \bar{1}$
a (Å)	7.30(1)	6.50	7.38	9.05	7.348	8.90
b (Å)	10.96(2)	7.37	20.13	10.88	9.771	11.56
c (Å)	11.70(2)	5.84	7.22	7.17	7.152	6.64
α, β, γ (°)	108(1), 102.1(4), 97.0(2)	$\beta = 108.38$		90.15, 90.58, 107	91.684, 98.523, 86.39	95.55, 90.52, 97.42
V (Å ³)	853(8)	265.49	1072.6	675.09	506.75	674.09
Z	6	2	8	2.2	2	4
Density (meas., calc.), g cm^{-3}	2.42, 2.43	2.5, 2.55	2.55, 2.48			2.189–2.286 (meas.)
Strongest lines of X-ray powder pat- terns, d (Å) – I	10.72 – 100 10.22 – 80 9.12 – 28 5.356 – 8 4.108 – 10 3.758 – 9 3.476 – 4	4.97 – 100 4.730 – 14 4.430 – 17 3.600 – 18 3.230 – 15 3.160 – 50 3.070 – 23 2.490 – 16 2.390 – 8	5.850 – 60 4.990 – 100 3.600 – 40 3.110 – 100 2.910 – 20 2.499 – 40 2.336 – 20 1.924 – 20 1.839 – 30 1.791 – 0	10.40 – 60 8.69 – 0 7.92 – 100 5.31 – 40 3.95 – 30 3.46 – 60 3.26 – 30 3.21 – 20 3.12 – 40	9.750 – 679 7.254 – 659 7.072 – 320 5.993 – 999 4.297 – 934 3.353 – 322 3.241 – 394 3.148 – 324 2.976 – 442 2.726 – 297	11.30 – 100 8.69 – 100 6.50 – 30 5.16 – 40 4.98 – 40 3.570 – 80 3.410 – 40 3.110 – 60 3.050 – 80 2.990 – 30

Table 3. (Contd.)

	$\text{Fe}(\text{SO}_4)(\text{OH}) \cdot 2\text{H}_2\text{O}$ This study	Butlerite (Anthony et al., 2003)	Parabutlerite (Anthony et al., 2003)	Hohmannite (Scordari, 1978)	Metahohmannite (Scordari et al., 2004)	Amarantite (Anthony et al., 2003)
Photo						
	Chemical composition (wt %)					
Fe_2O_3	37.82	38.96	39.42	34.42	40.75	35.91
SO_3	37.84	36.88	37.24	34.51	40.86	35.81
H_2O^+	22.70	$\text{H}_2\text{O}_{\text{calc.}}$ 21.51	$\text{H}_2\text{O}_{\text{calc.}}$ 21.75	31.06	18.39	28.28
SiO_2	0.26	0.18	0.05	—	—	—
Al_2O_3	0.38	0.04	0.05	—	—	—
Total	99.0	97.57	98.52	99.99	—	—
	Optical Properties					
α	1.596	1.593–1.604	1.589–1.598	1.559	1.709	1.516
β	?	1.665–1.674	1.660–1.663	1.643	1.718	1.598
γ	1.643	1.731–1.741	1.737–1.750	1.655	1.734	1.621
Optical sign, 2V		—	+, 43.5–87	—, 40	+, 70	—, 30

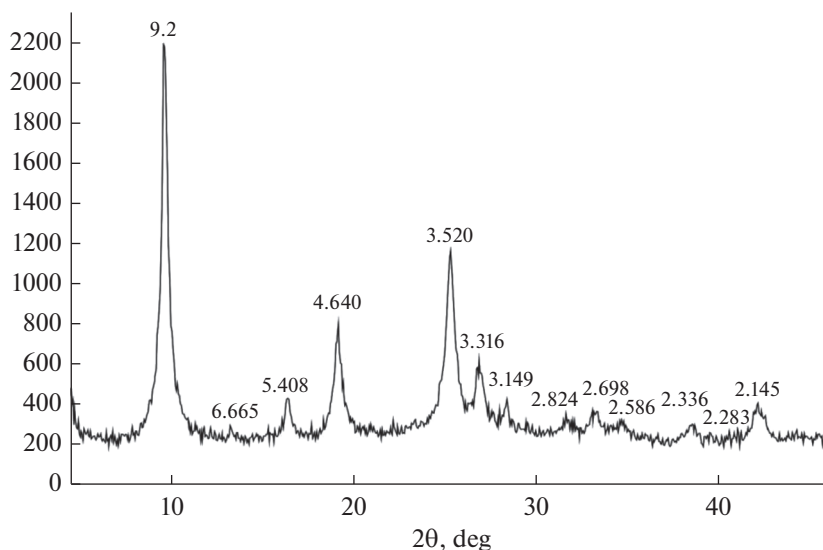


Fig. 12. X-ray powder patterns of the new phase occurring during calcination at 120 °C.

Рис. 12. Порошковая рентгенограмма новой фазы, проявленной при прокаливании до 120 °C.

thermal transformations in fibroferrite at 209 °C characterized by an X-ray diffraction pattern with a single strong reflection of 9.4 Å. When the temperature rises above 210 °C, the intermediate phase transforms into a new Fe(OH)(SO₄) phase. Ventruti et al. (2016a) insist that the compound they obtained is not a new polymorph of butlerite or parabutlerite. The sequence of transformations upon heating of butlerite and parabutlerite to 400 °C was studied by Majzlan et al. (2018). When heated to 160–200 °C, both minerals gradually lose crystallinity and become amorphous at temperatures above 200 °C. At a temperature of *ca.* 300 °C, the reflections of the Fe(SO₄)(OH) phase appear, becoming sharp at 400 °C. No new crystalline phases were recorded by Majzlan et al. (2018).

The process of thermal decomposition of our sulfate differs from that for butlerite and parabutlerite. When the mineral was heated up to 120–260 °C an unknown crystalline phase was formed for which the X-ray pattern is shown in Fig. 12. The Fe(SO₄)(OH) phase was recorded after calcination of the mineral at 345 °C. The Fe-dihydrate we have studied is characterized by a stable X-ray diffraction pattern with fairly strong reflections observed in the small-angle region, which differ from those given for the intermediate phase, recorded by Ventruti et al. (2016a).

CONCLUSIONS

Analyzing all the data obtained and comparing them with those known for hydrous ferric sulfates, we are inclined to believe that the mineral we found can be yet another polymorph of butlerite and parabutlerite and less stable. At this stage of investigation, without determining the crystal structure, one cannot give an unambiguous answer as to the position of this mineral within the group of known ferric sulfates.

The authors thank S.V. Krivovichev and the workers of the X-Ray Diffraction Centre of Saint Petersburg State University, O.V. Yakubovich (Moscow State University), N.V. Chukan-

ov (Institute of Problems of Chemical Physics RAS) for advice and assistance in the study. The authors are grateful to I.V. Klimova (Institute of Permafrost Science, SB RAS), as well as N.N. Emelyanova and T.I. Vasilieva (Diamond and Precious Metal Geology Institute, SB RAS) for help and interest in the work.

The work was done as part of State Assignment of DPMGI SB RAS and was partially funded by the Russian Science Foundation, under grant no. 18-35-00336.

REFERENCES

- Anthony J.W., Bideaux R.A., Bladh K.W., Nichols M.C. Handbook of Mineralogy. Miner. Soc. Amer., Chantilly, VA 20151-1110, USA, **2003**.
- Borene J. Structure crystalline de la parabutlerite. *Bull. Soc. Franc. Mineral. Cristallogr.* **1970**. Vol. 93. P. 185–189.
- Cejka J., Sejkora J., Plasil J., Bahfenne S., Palmer S.J., Rintoul L., Frost R.L. A vibrational spectroscopic study of hydrated Fe^{3+} hydroxyl-sulphates; polymorphic minerals butlerite and parabutlerite. *Spectroch. Acta Part A.* **2011**. Vol. 79(5). P. 1356–1363.
- Césbron F. Contribution à la Minéralogie des sulfates de fer hydratés. *Bull. Soc. franç. Minér. Crist.* **1964**. Vol. 87(2). P. 125–143.
- Fanfani L., Nunzi A., Zanazzi P.F. The crystal structure of butlerite. *Amer. Miner.* **1971**. Vol. 56. P. 751–757.
- Fridovsky V.Y. Structural control of orogenic gold deposits of the Verkhojansk-Kolyma folded region, northeast Russia. *Ore Geol. Rev.* **2018**. Vol. 103. P. 38–55.
- Fridovsky V.Yu., Kudrin M.V., Polufuntikova L.I. Multi-stage deformation of the Khangalas ore cluster (Verkhoyansk-Kolyma folded region, northeast Russia): ore-controlling reverse thrust faults and post-mineral strike-slip faults. *Minerals.* **2018**. Vol. 8(7). P. 270.
- Gamyarin G.N., Zayakina N.V., Galenchikova L.T. Arangasite, $\text{Al}_2(\text{PO}_4)(\text{SO}_4)\text{F} \cdot 7.5\text{H}_2\text{O}$, a new mineral from Alaskitovoe deposit (Eastern Yakutia, Russia). *Geol. Ore Deposits.* **2014**. Vol. 56. P. 560–566.
- Gamyarin G.N., Zhdanov Yu.Ya., Zayakina N.V., Gamyarina V.V., Suknev V.S. Mangazeite, $\text{Al}_2(\text{SO}_4)(\text{OH})_4 \cdot 3\text{H}_2\text{O}$ – a new mineral. *Geol. Ore Deposits.* **2007**. Vol. 49(7). P. 514–517.
- Hawthorne F.C., Krivovichev S.V., Burns P.C. The crystal chemistry of sulfate minerals. *Rev. Miner. Geochem.* **2000**. Vol. 40. P. 1–112.
- Kudrin M.V. The disseminated mineralization of the Khangalas gold deposit (Yana-Kolyma gold belt). In: *Proc. VIII Russian Youth Sci. Practic. School. New in the knowledge of ore formation processes.* Moscow, **2018**. P. 221–223 (in Russian).
- Kudrin M.V., Zayakina N.V., Vasileva T.I. Minerals of the oxidation zone of the Khangalas gold deposit (Eastern Yakutia). In: *Proc. VIII Russian Youth Sci. Practic. Conf. Geol. Mineral Resources of the North-East of Russia.* Yakutsk, **2018**. P. 77–80 (in Russian).
- Kudrin M.V., Vasileva T.I., Fridovsky V.Yu., Zayakina N.V., Polufuntikova L.I. Minerals of a weathering crust of the Khangalas ore cluster (North-East Russia). In: *Proc. IX Russian Youth Sci. Practic. Conf. Geol. Mineral Resources of the North-East of Russia.* Yakutsk, **2019**. P. 53–56 (in Russian).
- Lazebnik K.A., Zayakina N.V., Supletsov V.M. The first find of the rare mineral sanjuanite in Russia. *Dokl. Earth. Sci.* **1998**. Vol. 362. P. 233–235 (in Russian).
- Majzlan J., Dachs E., Benisek A., Plasil J., Sejkora J. Thermodynamics, crystal chemistry and structural complexity of the $\text{Fe}(\text{SO}_4)(\text{OH})(\text{H}_2\text{O})_x$ phases: $\text{Fe}(\text{SO}_4)(\text{OH})$, metahohmannite, butlerite, parabutlerite, amarantite, hohmannite, and fibroferrite. *Eur. J. Mineral.* **2018**. Vol. 30. P. 259–275.
- Scordari F. The crystal structure of hohmannite, $\text{Fe}_2(\text{H}_2\text{O})_4[(\text{SO}_4)_2\text{O}] \cdot 4\text{H}_2\text{O}$ and its relationship to amarantite, $\text{Fe}_2(\text{H}_2\text{O})_4[(\text{SO}_4)_2\text{O}] \cdot 3\text{H}_2\text{O}$. *Mineral. Mag.* **1978**. Vol. 42. P. 144–146.
- Scordari F. Fibroferrite: a mineral with a $\text{Fe}(\text{OH})(\text{H}_2\text{O})_2\text{SO}_4$ spiral chain and its relationship to $\text{Fe}(\text{OH})\text{SO}_4$, butlerite and parabutlerite, Tscher. *Mineral. Petrogr. Mitt.* **1981**. Vol. 28. P. 17–29.
- Scordari F., Ventruati G., Gualtieri A.F. The structure of metahohmannite, $\text{Fe}_2^{3+}[\text{O}(\text{SO}_4)_2] \cdot 4\text{H}_2\text{O}$, by in situ synchrotron powder diffraction. *Amer. Miner.* **2004**. Vol. 89. P. 365–370.
- Vasilieva T.I., Zayakina N.V. Modern mineral formation and seasonal minerals of the Endybal silver ore cluster (West Verkhoyanie, Yakutia). In: *Proc. IX Russian Youth Sci. Practic. Conf. Geology and Mineral Resources of the North-East of Russia.* Yakutsk, Russia, **2019**. P. 18–22 (in Russian).

Ventruti G., Ventura G.D., Orlando R., Scordari F. Structure refinement, hydrogen-bond system and vibrational spectroscopy of hohmannite, $\text{Fe}_2^{3+} [\text{O}(\text{SO}_4)_2] \cdot 8\text{H}_2\text{O}$. *Miner. Mag.* **2015**. V. 79. P. 11–24.

Ventruti G., Ventura G.D., Corriero N., Malferrari D., Gualtieri A.F., Susta U., Lacalamita M., Schingaro E. In situ high-temperature X-ray diffraction and spectroscopic study of fibroferrite, $\text{FeOH}(\text{SO}_4) \cdot 5\text{H}_2\text{O}$. *Phys. Chem. Miner.* **2016a**. V. 43. P. 587–595.

Ventruti G., Ventura G.D., Bellatreccia F., Lacalamita M., Schingaro E. Hydrogen bond system and vibrational spectroscopy of the iron sulfate fibroferrite, $\text{Fe}(\text{OH})\text{SO}_4 \cdot 5\text{H}_2\text{O}$. *Eur. J. Mineral.* **2016b**. V. 28. P. 943–952.

Yakubovich O.V., Steele I.M., Chernyshov V.V., Zayakina N.V., Gamyarin G.N., Karimova O.V. The crystal structure of arangasite, $\text{Al}_2\text{F}(\text{PO}_4)(\text{SO}_4)(\text{H}_2\text{O})_9$ determined using low-temperature synchrotron data. *Miner. Mag.* **2014**. V. 78(4). P. 889–903.

The RRUFF Project website containing an integrated database of Raman spectra, X-ray diffraction and chemistry data for minerals: <http://rruff.info/>, last access: February 25, **2015**.

Zayakina N. V. Cranswickite—a rare tetrahydrate sulfate of magnesium $\text{MgSO}_4 \cdot 4\text{H}_2\text{O}$, the new find in Yakutia. *Zapiski RMO (Proc. Russian Miner. Soc.)*. **2019**. N 1. P. 49–53 (in Russian).

ВОДНЫЙ СУЛЬФАТ ЖЕЛЕЗА $\text{Fe}(\text{SO}_4)(\text{OH}) \cdot 2\text{H}_2\text{O}$ ИЗ ЗОНЫ ГИПЕРГЕНЕЗА ЗОЛОТОРУДНОГО МЕСТОРОЖДЕНИЯ ХАНГАЛАС, ВОСТОЧНАЯ ЯКУТИЯ, РОССИЯ

д. чл. М. В. Кудрин^{а, *}, д. чл. Н. В. Заякина^а, В. Ю. Фридовский^а, Л. Т. Галенчикова^а

^аИнститут геологии алмаза и благородных металлов СО РАН, Якутск, Россия

*e-mail: kudrinmv@mail.ru

В зоне гипергенеза золоторудного месторождения Хангалас, Якутия, был обнаружен водный сульфат железа, не имеющий по результатам исследования аналогов среди природных и синтетических соединений. Минерал очень мягкой, бежево-желтого цвета с волокнистой текстурой и тонкокристаллической структурой. Встречается в виде прожилков и гнездообразных скоплений размером до 5–6 см в поперечнике, состоящих из очень мелких, тонких удлинённых, волокнистых кристаллов размерами ≤ 1 мкм в поперечнике и ≤ 20 мкм по удлинению. Ассоциирующие минералы: кварц, ярозит, мусковит и анортит. По данным химического анализа состав минерала следующий (классический мокрый химический анализ, мас. %): Fe_2O_3 37.82, SO_3 37.84, H_2O 22.70, SiO_2 0.26, Al_2O_3 0.38, сумма 99.0. Эмпирическая формула, рассчитанная на 1 атом S, — $\text{Fe}_{1.002}(\text{SO}_4)(\text{OH}) \cdot (\text{H}_{4.33}\text{O}_{2.18})$. Упрощенная формула — $\text{Fe}(\text{SO}_4)(\text{OH}) \cdot 2\text{H}_2\text{O}$, ей соответствует следующий состав (мас. %): Fe_2O_3 38.96, SO_3 39.07, H_2O 21.97, сумма 100.00. Параметры элементарной ячейки, уточненные по порошковой рентгенограмме: $a = 7.30(1)$, $b = 10.96(2)$, $c = 11.70(2)$ Å, $\alpha = 108(1)$, $\beta = 102.1(4)$, $\gamma = 97.0(2)^\circ$, $V = 853(8)$ Å³, $Z = 6$, триклинная сингония, вероятная пространственная группа $P1$, $P\bar{1}$ (?). Наиболее интенсивные линии на рентгенограмме [d , Å (I , %) (hkl): 10.72 (100) (001), 10.22 (80) (010), 9.12 (28) (0–11), 5.356 (8) (002), 4.108 (10) (–1–21), 3.758 (9) (1–22), 3.476 (4) (0–32)]. По химическому составу минерал близок природным полиморфам водного сульфата железа $\text{Fe}(\text{SO}_4)(\text{OH}) \cdot 2\text{H}_2\text{O}$ бутлериту и парабутлериту. Однако он отличается от них по рентгенограмме, ИК и рамановским спектрам. Этот факт послужил основанием для детального исследования минерала. Из-за тонковолокнистого строения и плохого качества рентгеновских дифракционных отражений кристаллическая структура обнаруженного сульфата не расшифрована. В основном по этой причине минерал не был утвержден Комиссией по новым минералам Международной минералогической организации (CNMMN IMA).

Ключевые слова: водный сульфат железа, $\text{Fe}(\text{SO}_4)(\text{OH}) \cdot 2\text{H}_2\text{O}$, бутлерит, парабутлерит, порошковая рентгенограмма, ИК-спектр, рамановский спектр, зона гипергенеза, мерзлота, месторождение Хангалас, Якутия

СПИСОК ЛИТЕРАТУРЫ

Васильева Т.И., Заякина Н.В. Современное минералообразование и сезонные минералы Эндыбальского серебрянорудного узла (Западное Верхоянье, Якутия) / Мат. IX Всероссийск. научно-практич. конф. “Геология и минерально-сырьевые ресурсы северо-востока России”. Якутск, **2018**. С. 18–22.

Заякина Н.В. Крансвикит – редкий четырехводный сульфат магния $\text{MgSO}_4 \cdot 4\text{H}_2\text{O}$, новая находка в Якутии // ЗРМО. **2019**. Т. 148. № 1. С. 49–53.

Кудрин М.В. Вкрапленная минерализация золоторудного месторождения Хангалас (Яно-Колымский золотоносный пояс) / Мат. 8-й Российской молодежной научно-практич. школы “Новое в познании процессов рудообразования”. Москва, **2018**. С. 221–223.

Кудрин М.В., Заякина Н.В., Васильева Т.И. Минералы зоны окисления золоторудного месторождения Хангалас (Восточная Якутия) / Мат. VIII Всероссийск. научно-практич. конф. “Геология и минерально-сырьевые ресурсы северо-востока России”. Якутск, **2018**. С. 77–80.

Кудрин М.В., Васильева Т.И., Фридовский В.Ю., Заякина Н.В., Полуфунтикова Л.И. Минералы коры выветривания Хангаласского рудного узла (северо-восток России) / Мат. IX Всероссийск. научно-практич. конф. “Геология и минерально-сырьевые ресурсы северо-востока России”. Якутск, **2019**. С. 53–56.

Лазебник К.А., Заякина Н.В., Суплецов В.М. Первая находка в России редкого минерала санхунита // Докл. РАН. **1998**. Т. 362. № 2. С. 233–235.